A 2D UNSTRUCTURED DAM-BREAK MODEL: FORMULATION AND VALIDATION

Xinya Ying[*1], Jeff Jorgeson[2], and Sam S. Y. Wang[1]

[1] National Center for Computational Hydroscience and Engineering, The University of Mississippi University, Mississippi, 38677

[2] U.S. Army Engineer Research and Development Center, Coastal and Hydraulics Laboratory Vicksburg, Mississippi, 39018

ABSTRACT

Two-dimensional simulations of dam-break flows using finite volume method and approximate Riemann solvers for computing the intercell fluxes have drawn growing attentions because of their robustness and abilities to handle mixed flows and discontinuities. Such models usually require complicated algorithms for treating source terms and second-order schemes for computing the intercell fluxes in order to gain numerically balanced solutions and accuracy, which often results in an excessively long computational time. With a view of developing an accurate and efficient model for real-life applications, this paper proposed a finite volume method, which uses the first-order HLL approximate Riemann solver for computing intercell fluxes and adopts the conservative form of the momentum equations with one source term representing the driving forces in each equation. Such treatment can easily eliminate numerical imbalance between source and flux terms without introducing complicated algorithms. The accuracy and improvement in computational efficiency of the newly developed model are demonstrated by means of a real-life test example.

1. INTRODUCTION

The catastrophic failure of a dam often causes widespread downstream flooding, which may directly affect mobility, deployment, and safety of the army. A 2D dam-break model can capture both spatial and temporal evolution of a potential dam-break flood event and provide sufficient details on the flood, such as flood depths, flow velocities, and timing of the flood arrival and recession at specific locations and times. Such pieces of information are crucial for military planning in the areas having potential dam-break risk.

Numerical solution of two-dimensional dam-break flows has been a great challenge to hydraulic engineers and researchers, because it often involves complex geometry, mixed flow regimes, and discontinuities. Among numerous approaches, the use of finite volume method with unstructured grid and approximate Riemann solvers for computing the intercell fluxes has gained increasing popularity, because of its highly adaptive ability to complex geometry, robustness, abilities to handle mixed flows and discontinuities, and outstanding mass conservation property (e.g., Zhao et al. 1996; Brufau and Garcia-Navarro 2000; Valiani et al. 2002; Yoon and Kang 2004). However, when source terms are presented due to uneven bathymetry, such methods may create numerical imbalance because of the artificial splitting of driving forces in the governing equations between flux and source terms, which are then evaluated using different methods. Such numerical imbalance can lead an unphysical flow even in a still water test case, as illustrated by Rogers et al (2003) through a two-dimensional simulation of a circular water basin with uneven bathymetry. So far, many researchers have attempted to overcome these problems. For example, Nujic (1995) adopted the form of the governing equation in which the hydrostatic pressure force term is extracted from the flux. Such treatment makes it possible to discretize two source terms using the same method and thus to satisfy the numerical balance. Zhou et al. (2001) proposed the surface gradient method (SGM) for the treatment of the source terms. In the SGM, water depth at left and right of the interfaces is evaluated based on the linear reconstruction of water surface level. This method can eliminate numerical imbalance problem without introducing a complex algorithm for the source terms. Rogers et al (2003) used an algebraic approach in which the governing hyperbolic system of conservation laws is reformulated in terms of deviations away from an unforced but separately specified equilibrium state and the numerical balancing is achieved by incorporating the resulting extra physical information.

The use of complicated algorithms for treating source terms and the second-order schemes for computing the intercell fluxes often result in an excessively long computational time (e.g., Valiani et al. 2002; Yoon and Kang 2004). In the case of a large scale problem, the cost of computational time can be prohibitive. With a view of developing an accurate and efficient model for real-life applications, Ying et al (2006) proposed a finite volume

Report Documentation Page

Form Approved
OMB No. 0704-0188

1. REPORT DATE	2. REPORT TYPE	3. DATES COVERED
01 NOV 2006	**N/A**	**-**

4. TITLE AND SUBTITLE	5a. CONTRACT NUMBER
A 2D Unstructured Dam-Break Model: Formulation And Validation	5b. GRANT NUMBER
	5c. PROGRAM ELEMENT NUMBER
6. AUTHOR(S)	5d. PROJECT NUMBER
	5e. TASK NUMBER
	5f. WORK UNIT NUMBER
7. PERFORMING ORGANIZATION NAME(S) AND ADDRESS(ES) **National Center for Computational Hydroscience and Engineering, The University of Mississippi University, Mississippi, 38677**	8. PERFORMING ORGANIZATION REPORT NUMBER
9. SPONSORING/MONITORING AGENCY NAME(S) AND ADDRESS(ES)	10. SPONSOR/MONITOR'S ACRONYM(S)
	11. SPONSOR/MONITOR'S REPORT NUMBER(S)

12. DISTRIBUTION/AVAILABILITY STATEMENT
Approved for public release, distribution unlimited

13. SUPPLEMENTARY NOTES
See also ADM002075., The original document contains color images.

14. ABSTRACT

15. SUBJECT TERMS

16. SECURITY CLASSIFICATION OF:			17. LIMITATION OF ABSTRACT	18. NUMBER OF PAGES	19a. NAME OF RESPONSIBLE PERSON
a. REPORT	b. ABSTRACT	c. THIS PAGE			
unclassified	**unclassified**	**unclassified**	**UU**	**6**	

method, which uses the first-order HLL approximate Riemann solver for computing intercell fluxes and adopts the conservative form of the momentum equations with one source term representing the driving forces in each equation. Such treatment can easily eliminate numerical imbalance between source and flux terms without introducing complicated algorithms, and thus increase computational efficiency. Numerical tests have shown that this method is able to satisfactorily predict oblique hydraulic jump and partial dam-break flow (Ying et al. 2006). In this paper, a real-life test example with complex geometry (Malpasset dam-break case) is used to further demonstrate the accuracy and improvement in computational efficiency of this newly proposed method.

2. GOVERNING EQUATIONS

The two-dimensional shallow water equations are obtained by integrating the Navier-Stokes equations over the flow depth based on several assumptions such as hydrostatic pressure distribution and small bottom slope. The equations in conservation and vector form are written as

$$\frac{\partial \mathbf{U}}{\partial t} + \frac{\partial \mathbf{E}}{\partial x} + \frac{\partial \mathbf{G}}{\partial y} = \mathbf{S} \tag{1}$$

in which, **U, E(U), G(U)** and **S(U)** are respectively the vectors of conserved variables, fluxes in the x and y direction, and sources, defined as follows.

$$\mathbf{U} = \begin{bmatrix} h \\ hu \\ hv \end{bmatrix} \qquad \mathbf{E} = \begin{bmatrix} hu \\ huu \\ huv \end{bmatrix} \qquad \mathbf{G} = \begin{bmatrix} hv \\ huv \\ hvv \end{bmatrix}$$

$$\mathbf{S} = \begin{bmatrix} 0 \\ -gh\dfrac{\partial Z}{\partial x} - g\dfrac{n^2 u\sqrt{u^2+v^2}}{h^{1/3}} \\ -gh\dfrac{\partial Z}{\partial y} - g\dfrac{n^2 v\sqrt{u^2+v^2}}{h^{1/3}} \end{bmatrix}$$

where h = water depth; u and v = velocity component in the x and y direction, respectively; g = gravitational acceleration; Z = water level; n = Manning's coefficient.

For convenience, Eq. (1) is often rewritten as

$$\frac{\partial \mathbf{U}}{\partial t} + \nabla \cdot \mathbf{F} = \mathbf{S} \tag{2}$$

where $\mathbf{F} = \mathbf{E}\,\vec{i} + \mathbf{G}\,\vec{j}$

In the above form of the Saint Venant equations, the driving forces are represented by only one term with the water surface gradient, which makes it very nice for treating the source term because: (1) the variation of water surface is generally much smoother than water depth and bottom; (2) it eliminates numerical imbalance that arises due to using different methods to evaluate driving forces that are split between the flux and the source terms. As a matter of fact, Nujic (1995) proposed a balancing technique in which the pressure term due to water depth is extracted from the flux and combined into the bottom slope term, which actually resulted in the same form of the governing equation as Eq. (1).

3. NUMERICAL METHOD

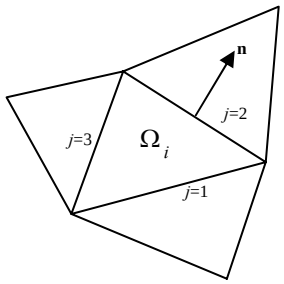

Fig. 1 Diagram for control volume definition

The governing equations are discretized according to the cell centered finite volume method on a triangular grid, as shown in Fig. 1. The conserved variables are defined at the cell centers and represent the average value over each cell, while the fluxes are calculated at the interfaces between cells.

Integrating Eq. (2) over the i^{th} cell, one obtains

$$\int_{\Omega_i} \frac{\partial \mathbf{U}}{\partial t}\, d\Omega + \int_{\Omega_i} \nabla \cdot \mathbf{F}\, d\Omega = \int_{\Omega_i} \mathbf{S}\, d\Omega \tag{3}$$

where Ω_i = the area of the i^{th} cell. Applying Green's theorem to the second term in Eq. (3) yields

$$\int_{\Omega_i} \frac{\partial \mathbf{U}}{\partial t}\, d\Omega + \oint_{\Gamma_i} \mathbf{F} \cdot \mathbf{n}\, d\Gamma = \int_{\Omega_i} \mathbf{S}\, d\Omega \tag{4}$$

where Γ_i = boundary of the i^{th} cell and $\mathbf{n}$ = the unit outward vector normal to the boundary. The second term in Eq. (4) can be approximated as

$$\oint_{\Gamma_i} \mathbf{F} \cdot \mathbf{n}\, d\Gamma = \sum_{j=1}^{3} \mathbf{F}_{ij} \cdot \mathbf{n}_{ij}\, \Delta\Gamma_{ij} \tag{5}$$

where the subscripts i and j denote the i^{th} cell and the j^{th} edge of the cell, respectively; $\Delta\Gamma$ = the length of an edge of a triangular cell.

Therefore, Eq. (4) can be written as

$$\frac{\mathbf{U}_i^{n+1}-\mathbf{U}_i^n}{\Delta t}=-\frac{1}{\Omega_i}\sum_{j=1}^{3}\mathbf{F}_{ij}\cdot\mathbf{n}_{ij}\,\Delta\Gamma_{ij}+\mathbf{S}_i \tag{6}$$

According to Godunov (1959), the variables are approximated as constant states within each cell and then the fluxes at interfaces are calculated by solving resultant Riemann problems that exist at interfaces. In the present model, the HLL approximate Riemann solver, proposed by Harten, Lax and van Leer (Harten et al. 1983), is used to calculate the intercell flux, because of its robustness and ease to implement. According to the HLL Riemann solver, the intercell flux is given by

$$\mathbf{F}_{ij}\cdot\mathbf{n}_{ij}=\begin{cases}(\mathbf{F}_{\mathrm{L}})_{ij}\cdot\mathbf{n}_{ij} & (\text{if } S_{\mathrm{L}}\ge 0)\\ \dfrac{S_{\mathrm{R}}(\mathbf{F}_{\mathrm{L}})_{ij}\cdot\mathbf{n}_{ij}-S_{\mathrm{L}}(\mathbf{F}_{\mathrm{R}})_{ij}\cdot\mathbf{n}_{ij}+S_{\mathrm{R}}S_{\mathrm{L}}[(\mathbf{U}_{\mathrm{R}})_{ij}-(\mathbf{U}_{\mathrm{L}})_{ij}]}{S_{\mathrm{R}}-S_{\mathrm{L}}} & (\text{if } S_{\mathrm{L}}\le 0\le S_{\mathrm{R}})\\ (\mathbf{F}_{\mathrm{R}})_{ij}\cdot\mathbf{n}_{ij} & (\text{if } S_{\mathrm{R}}\le 0)\end{cases} \tag{7}$$

where $\mathbf{U}_{\mathrm{L}}$ and $\mathbf{U}_{\mathrm{R}}$ are conserved variables of the left and right states, respectively; and S_{L} and S_{R} are left and right traveling wave speeds, respectively, which are estimated according to the following equations (Fraccarollo and Toro 1995).

$$S_{\mathrm{L}}=\min\left(V_{\mathrm{L}}-\sqrt{gh_{\mathrm{L}}},V^*-\sqrt{gh^*}\right) \tag{8}$$

$$S_{\mathrm{R}}=\max\left(V_{\mathrm{R}}+\sqrt{gh_{\mathrm{R}}},V^*+\sqrt{gh^*}\right) \tag{9}$$

where V_{L} and V_{R} are respectively the velocity components of the left and the right states in the unit vector $\mathbf{n}$ direction; h_{L} and h_{R} are water depth of the left and the right states, respectively.

$$V^*=\frac{1}{2}\left(V_{\mathrm{L}}+V_{\mathrm{R}}\right)+\sqrt{gh_{\mathrm{L}}}-\sqrt{gh_{\mathrm{R}}} \tag{10}$$

$$\sqrt{gh^*}=\frac{1}{2}\left(\sqrt{gh_{\mathrm{L}}}+\sqrt{gh_{\mathrm{R}}}\right)+\frac{1}{4}\left(V_{\mathrm{L}}-V_{\mathrm{R}}\right) \tag{11}$$

Note that for a dry bed problem the wave speeds S_L and S_{R} are estimated according to the following expressions.

$$S_{\mathrm{L}}=V_{\mathrm{L}}-\sqrt{gh_{\mathrm{L}}}\ ,\quad S_{\mathrm{R}}=V_{\mathrm{L}}+2\sqrt{gh_{\mathrm{L}}}\quad\text{(for right dry bed)} \tag{12}$$

$$S_{\mathrm{L}}=V_{\mathrm{R}}-2\sqrt{gh_{\mathrm{R}}}\ ,\ S_{\mathrm{R}}=V_{\mathrm{R}}+\sqrt{gh_{\mathrm{R}}}\quad\text{(for left dry bed)} \tag{13}$$

Water surface gradients in the source term are evaluated by

$$\frac{\partial Z}{\partial x}=\frac{1}{\Omega_i}\oint_{\Gamma_i}Z dy\ ,\quad \frac{\partial Z}{\partial y}=\frac{1}{\Omega_i}\oint_{\Gamma_i}Z dx \tag{14}$$

It is easy to see that the resulting scheme does not cause numerically generated flow or numerical imbalance problem. Let us consider an open channel filled with water at rest. Obviously, the water will remain at rest if no disturbance is applied to the domain and boundaries. If we apply above scheme to simulate this case, we can see the source terms, including water surface gradient term and friction term, and flux terms in Eq. (4) are exactly equal to zero at initial time, no matter how bed elevation changes. As a result, the solutions of Z and Q at succeeding time will remain the same as initial state, in other words, no flow is numerically generated.

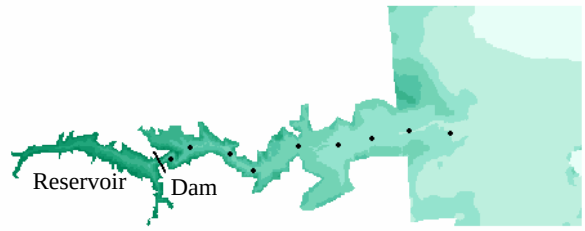

Fig. 2 Topography and locations of measuring points for Malpasset dam-break case

4. MODEL VALIDATIONS USING MALPASSET DAM-BREAK CASE

4.1 Malpasset Dam-Break Event

The Malpasset dam was located in a narrow gorge of the Reyran river valley in France. It was a 66.5 m high arch dam with a crest length of 223 m and the maximum reservoir capacity of 55×10^6 m^3. In the immediate downstream of the dam, the Reyran river valley is very narrow and has two consecutive sharp bends. Then the valley widens as it goes downstream and eventually reaches the flat plain (see Fig. 2). The dam failed in 1959 following an exceptionally heavy rain. After the dam failure, a field survey was performed to obtain the maximum water levels along the Reyran river valley. In addition, a physical model with a scale of 1/400 was built to study the dam-break flow in 1964. The maximum water level and the flood wave arrival time at 9 points along the river valley were measured (see Fig.2). Because of its complex topography and availability of measured data, the Malpasset dam-break case was selected as a benchmark test example for dam-break models in the CADAM project (Goutal 1999). More

detailed descriptions about the Malpasset dam-break test case can be found in literature (e.g. Goutal 1999, Hervouet 2000, and Valiani et al. 2002).

4.2 Numerical Simulations

In the computations, two distinct triangular meshes were respectively used in order to investigate the impact of mesh size on the modeling results. Mesh A, as shown in Fig.3, is composed of 26000 cells and highly refined at the dam site, the immediately downstream valley, and along the downstream river, which allows the model accurately capture the details on flooding. Mesh B, as shown in Fig.4, is composed of 8835 cells and not excessively refined in order to increase computational efficiency. It should be noted that Mesh A was directly adopted from the CADAM project and Mesh B was generated by the commercial software SMS. The initial water level in the reservoir was set to be 100 m above sea level. The rest of the computational domain was considered as dry bed. The previous study has shown that the initial downstream river flow is negligible because of its relatively small flow rate comparing to the flow caused by the dam failure (Hervouet 2000). The Manning's coefficient was set to be 0.025 $m^{-1/3}s$ over the entire computational domain. The time interval Δt = 0.025 s for Mesh A and Δt = 0.06 s for Mesh B. The calculations with a final time t = 3000s require 1 hour 5 minutes for the Mesh A and 7.6 minutes for the Mesh B on a PC with AMD 2.4 GHz CPU.

4.3 Result and Analysis

Figs.5 and 6 show the flooded area and water depth, calculated using Mesh A and Mesh B, respectively. It is observed that the overall flooded area and water depth obtained from Mesh A and Mesh B are very similar, despite some tiny and local differences in flooded area and water depth. It is not surprising there are such differences, because Mesh B is much coarser than Mesh A so that some fine topographic details such as downstream river are not well represented in the simulation using Mesh B.

Figs. 7 and 8 compare the computed maximum water level and wave front arrival time with the measured data. In these figures, good agreements between Mesh A's and Mesh B's results are observed again. Fig. 7 also shows that the results of maximum water level from the present model are very close to those from the model developed by Valiani et al. (2002), in which the high order schemes were used for both estimating intercell fluxes and time advancing. It is important to note that their calculation on a quadrangular mesh with 10696 cells requires 26 hours on a PC with Pentium III 700 MHz CPU, whereas the present model using Mesh A (26000 cells) only requires 4 hours 11 minutes of computational time on a PC with similar performance (Pentium III 850 MHz CPU). This indicates that the present model can substantially increase computational efficiency, while accuracy is preserved.

5. CONCLUSIONS

A two-dimensional dam-break model has been developed based on finite volume method using unstructured grids. The intercell fluxes are evaluated based on the HLL approximate Riemann solver. The momentum equation used in the model has only one source term representing the driving forces. This approach can successfully eliminate the numerical imbalance between source and flux terms. The model is validated against laboratory data from a real-life dam-break case. The results show that the simulations using either Mesh A or Mesh B are capable of correctly capturing major hydrodynamic behaviors of the flood event, such as maximum water level and wave front arrival time. The comparison of computational times with other models further demonstrates that the present model is more efficient than conventional unstructured models using high-order schemes for estimating fluxes and complicated upwind algorithms for treatment of source term. Such an unstructured model allows using arbitrary computational domain and meshes with local refinement. This provides the more efficient way to obtain local fine details on flooding than structured models.

To sum up, the proposed model is able to correctly capture both spatial and temporal evolution of a potential dam-break flood event and provide crucial information for military planning in the areas having potential dam-break risk.

ACKNOWLEDGEMENTS

This work is a result of research sponsored by the USDA Agriculture Research Service under Specific Research Agreement No. 58-6408-2-0062 (monitored by the USDA-ARS National Sedimentation Laboratory), U.S. Army Research Office under Grant # W911NF-04-1-0048, and The University of Mississippi. The authors wish to thank Dr. Sandra Soares Frazao (University Catholique de Louvain) for providing valuable data set of the Malpasset dam-break case.

REFERENCES

Godunov, S.K., 1959: Finite Difference Method for Numerical Computation of Discontinuous

Solutions of the Equations of Fluid Dynamics, *Math. Sbonik,* 47(3), 271-306 (in Russian).

Goutal, N., 1999: The Malpasset Dam Failure – An Overview and Test Case Definition, The Proceeding of the 4th CADAM meeting, Nov. 18-19, Zaragoza, Spain.

Harten A., Lax P.D., and Van Leer, B., 1983: On Upstream Differencing And Godunov-Type Schemes For Hyperbolic Conservation Laws, *SIAM Review*, 25(1), 35-61.

Hervouet J.M., 2000: A High Resolution 2-D Dam-Break Model Using Parallelization, *Hydrological Processes 2000*, 14, 2211-2230.

Valiani, A., Caleffi, V. and Zanni, A., 2002: Case Study: Malpasset Dam-Break Simulation Using A Two-Dimensional Finite Volume Method, *J. Hydraulic Engineering*, ASCE, 128(5), 460-472.

Brufau, P. and Garcia-Navarro, P., 2000: Two-Dimensional Dam Break Flow Simulation, *Int. J. Numer. Meth. Fluids*, 33, 35-57.

Nujic, M., 1995: Efficient Implementation Of Non-Oscillatory Schemes For The Computation Of Free-Surface Flows, *J. of Hydraul. Res*. 33 (1), 100-111.

Rogers, B.D., Borthwick, A.G.L. and Taylor, P. H., 2003: Mathematical Balancing Of Flux Gradient And Source Terms Prior To Using Roe's Approximate Riemann Solver, *J. Comput. Phys*. 192, 422-451.

Ying, X., Jorgeson, J. and Wang, S.Y., 2006: Two-dimensional Flood Simulation on Unstructured Grids, *Proceeding of ASCE World Water and Environmental Resources Congress 2006*, May 21-25, Omaha, Nebraska

Yoon, T.H. and Kang S.K., 2004: Finite Volume Model For Two-Dimensional Shallow Water Flows On Unstructured Grids, *J. Hydraulic Engineering,* 130(7), 678-688.

Zhou, J.G., Causon, D.M., Mingham, C.G. and Ingram, D.M., 2001: The Surface Gradient Method For The Treatment Of Source Terms In The Shallow-Water Equations, *J. Comput. Phys.* 168, 1-25.

Zhao, D. H., Shen, H.W., Lai, J.S., and Tabios III, G.Q., 1996: Approximate Riemann Solvers In FVM For 2D Hydraulic Shock Wave Modeling, *J. Hydraulic Engineering*, ASCE, 122(12), 692-702.

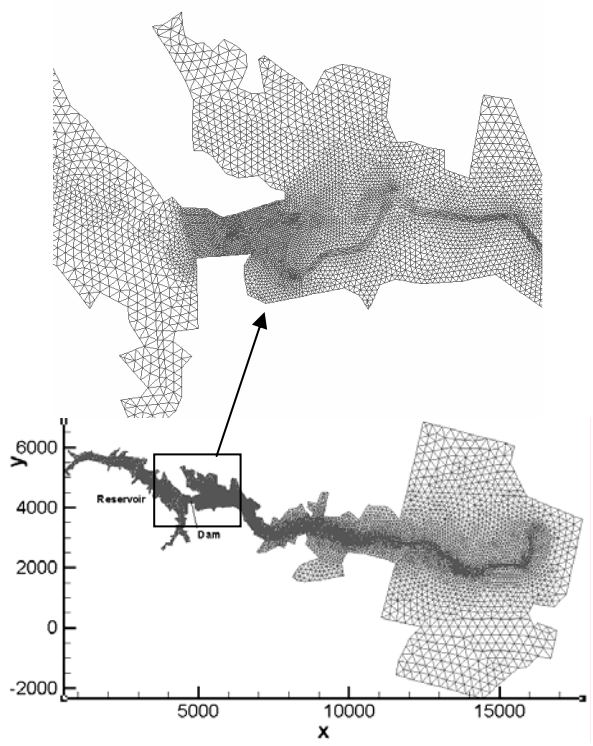

Fig. 3 Mesh A used for simulation

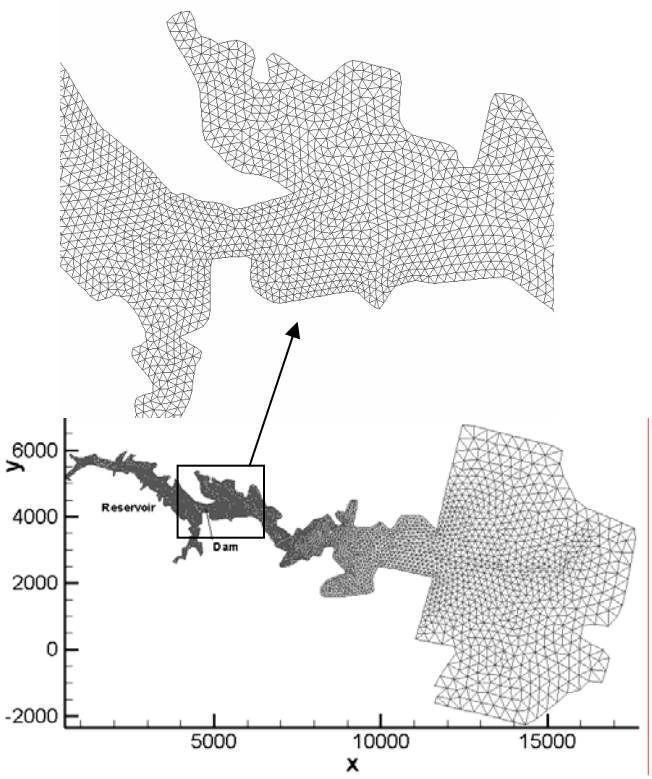

Fig. 4 Mesh B used for simulation

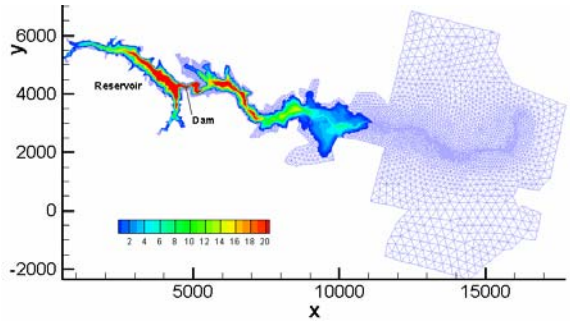

(a) t = 800 s

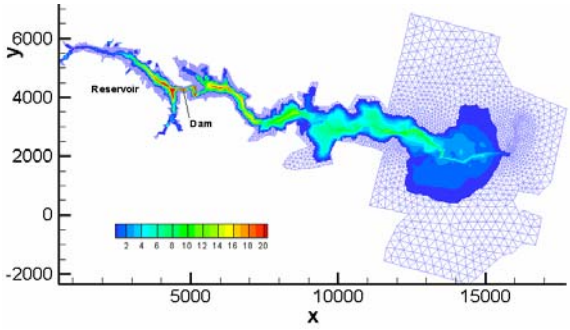

(b) t = 1800 s

Fig. 5 Water depth computed using Mesh A

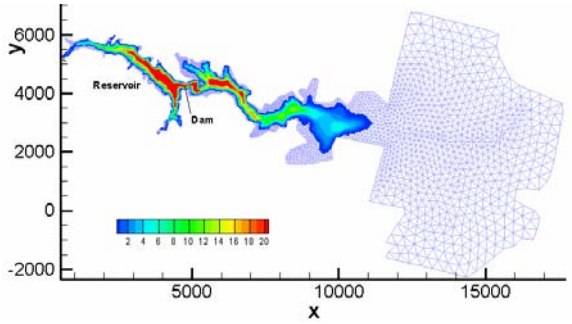

(a) t = 800 s

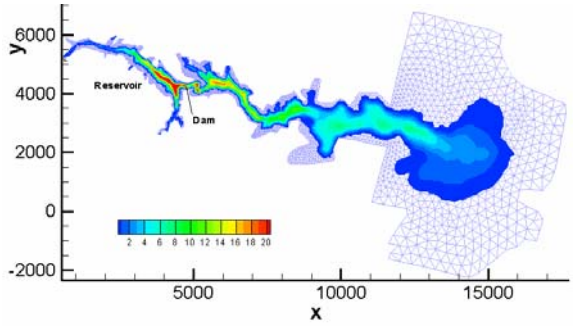

(b) t = 1800 s

Fig. 6 Water depth computed using Mesh B

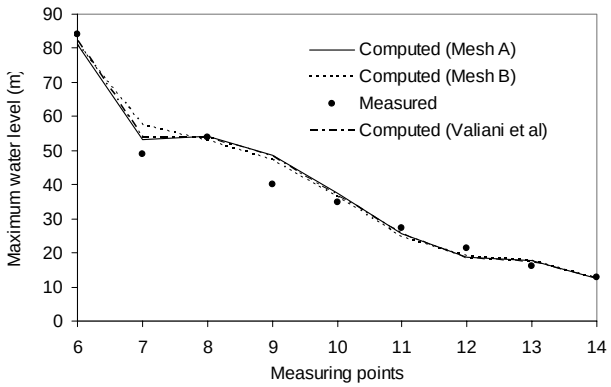

Fig. 7 Comparison of computed maximum water level with measured data from physical model

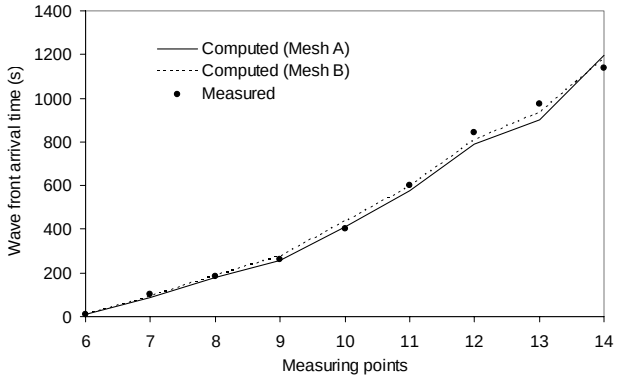

Fig. 8 Comparison of computed wave front arrival time with measured data from physical model